Physical Science International Journal

24(3): 20-42, 2020; Article no.PSIJ.56687
ISSN: 2348-0130

Seepage and Recharge under a Stream-aquifer Unsaturated Connection

Hubert J. Morel-Seytoux[1*]

[1]Hydroprose International Consulting, 684 Benicia Drive Unit 71, Santa Rosa, CA 95409, United States of America.

Author's contribution

The sole author designed, analysed, interpreted and prepared the manuscript.

Article Information

DOI: 10.9734/PSIJ/2020/v24i330181
Editor(s):
(1) Dr. Humaira Yasmin, King Faisal University, Saudi Arabia.
(2) Dr. Thomas F. George, University of Missouri-St. Louis, USA.
Reviewers:
(1) Xinyu Liu, Hohai University, China.
(2) Atul Kumar Srivatava, Central University of Jharkhand, India.
Complete Peer review History: http://www.sdiarticle4.com/review-history/56687

Original Research Article

Received 01 March 2020
Accepted 06 May 2020
Published 20 May 2020

ABSTRACT

Most widely used integrated hydrologic models use outdated descriptions of the stream-aquifer flow exchange. Understandably they do it for practical reasons to avoid computational costs in large-scale regional studies. In this article we propose a largely analytical technique that (1) describes the situation when the connection is unsaturated while avoiding a lot of numerical work and at the same time remains quite physical, (2) has the capability to describe fluctuations between saturated and unsaturated connections, and (3) can be coupled easily with the numerical groundwater model that describes what happens in the broad system of cells away from the river(s). Essentially two separate methods are compared for the purpose of selecting the most practical of the two.

Keywords: Stream-aquifer interaction; flow exchange; stream depletion; saturated or unsaturated hydraulic connection; analytical coupling.

1. BACKGROUND INTRODUCTION

In the United States the development of most groundwater (or integrated hydrologic) simulation models in wide use today for large-scale regional studies was initiated some 60-70 years ago. Then models such as MODFLOW [1] tried to be as rigorous and physically based as possible. However at the time computer storage and power were limited. Out of necessity the mathematical models had to greatly simplify a complex reality and as a result

**Corresponding author: E-mail: hydroprose@sonic.net;*

the models ended up highly conceptual in some places.

Discussion of the limitations of MODFLOW to estimate the seepage flow between a stream and a water-table aquifer, whether in saturated or unsaturated connection, are provided in a number of publications [2,3].

At that time the United States' interest in water, in its availability and purity, was fairly limited. It was not until the Water Resources Research Act was passed in 1964 that substantial financial support became available for research in the general field of water. Great improvements were then implemented in the following decades with use of more powerful computers, GIS and numerous other technologies. Yet for some components the original empirical approaches have remained unchanged.

Nowadays however concern for the availability of water under simultaneous conditions of climate change and continued growth of population has greatly increased. This is evident in California. The "Sustainable Groundwater Management Act", SGMA, passed on September 16, 2014, requires that new agencies, Sustainable Groundwater Agencies, SGA, be created in all groundwater basins. These new agencies, which had to be created by June 30, 2017, must provide the Department of Water Resources by January 31, 2022 a plan that would show that the SGA has taken action for sustainability of the groundwater resource. The majority of these plans will be supported by simulations with groundwater models.

Back in the early 1970s days, with limited computer capability, it was customary to assume that the flow in the water-table aquifer was essentially horizontal (the Dupuit-Forchheimer, DF, assumption). Given that assumption the groundwater flow equation to be solved for the large system was two-dimensional in a horizontal plane since there was no vertical flow. The obvious purpose was not to have to deal numerically with a three-dimensional problem size.

However it is very clear that in the vicinity of a river's cross-section the flow is not horizontal. Fig. 1 illustrates that point where flow lines are shown for a river with rectangular cross-section. These flow lines were obtained with a numerical code using a very fine grid under a steady-state condition. The flow in the aquifer does not become horizontal until a significant distance away from the banks of the river, where the equipotential (constant head) lines become essentially vertical.

However the size of the space where the flow is not horizontal is small relative to the size of the finite difference cells in the large-scale region. It was wasteful to have to solve a three-dimensional system of equations when as a whole it was necessary only over a limited domain. Thus the idea came to couple an analytical solution in a vertical plane with the two-dimensional system of equations in the horizontal plane. For different cross-section shapes (elliptical, triangular, rectangular, trapezoidal) such analytical solutions were found. The problem was then ,deduced from the analytical solutions, to estimate a dimensionless conductance of the big streamtube from the river's wetted perimeter to a location where the head in the aquifer satisfied the assumption that flow was horizontal. At the right and left boundaries of Fig. 1 the potential (constant head) lines are vertical.

Fig. 1 shows many small streamtubes. The resistance to flow in each of these streamtubes is quite different. It is relatively small for the top streamtubes, where flow is almost linear. It is much larger for the bottom ones where the geometry of flow is complex, involving zones of divergence and convergence and significant curvature. The task was to find the conductance of the overall streamtube, the composite of all the small streamtubes. That task was successful over a decade long sustained effort [2,4] Once a value for the dimensionless conductance, Γ, **considering only one side**, was obtained then one could estimate the one-sided seepage discharge in the case of saturated flow as:

$$Q_{one-sided} = \Gamma L_R K_H (h_S - h_{DF}) \qquad (1)$$

L_R is the length of the river within the aquifer cell that contains the river , K_H is the aquifer horizontal conductivity, h_S is the head in the river and h_{DF} is the head in the aquifer at a distance such that by that location the flow has become horizontal, referred also as the far distance h_{far}. h_{DF} is the head calculated by the solution of the two-dimensional groundwater equations in the horizontal plane.

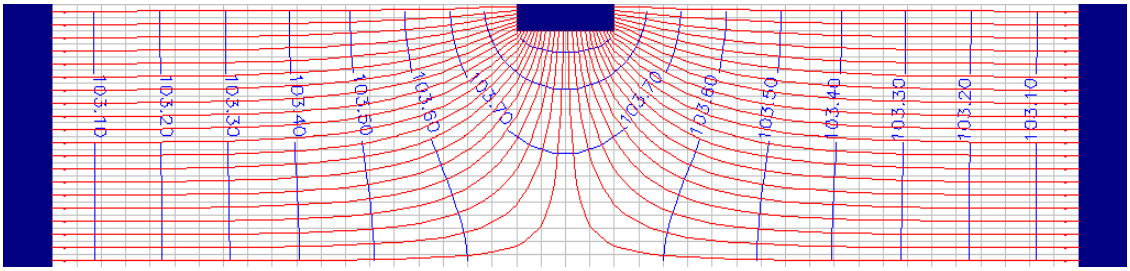

Fig. 1. View of seepage from the river to the aquifer in a vertical cross-section

It was then possible to link an essentially two-dimensional analytical vertical model to a numerical two-dimensional groundwater model in the horizontal plane. This resulted in an effective 3-dimensional model without the heavy burden to do it entirely numerically.

Following this somewhat lengthy explanation of the background needed to understand the additional research to be presented, it is time to state the purpose of this article. The main purpose of this article is to address the case of unsaturated connection between the river and the water-table below the riverbed. Whereas the numerical solution of the saturated groundwater flow equations is relatively simple that for unsaturated flow is significantly more complicated, being highly nonlinear.

To avoid those difficulties, two approximate analytical methods of solution for the description of the unsaturated zone water content profile below a tight riverbed (clogging layer) have been developed. The first developed method has (1) the disadvantage of requiring one numerical integration and (2) to be limited to a few values of the parameters that characterize the relative conductivity and capillary pressure of the aquifer porous medium. The second method avoids both these limitations but may appear less realistic. A comparison of the two methods on a common set of data is presented to verify that they give essentially the same results.

2. GENERAL APPROACH TO SOLVE THE CASE OF UNSATURATED CONNECTION

The first issue to consider is under what condition does unsaturated connection start when until then the connection was saturated? The initial time at which desaturation starts is termed *incipient desaturation*, and in reverse *incipient resaturation*.

Once an unsaturated connection is established the system includes one more zone, the unsaturated zone. The physical system now consists of the river, a clogging layer, an unsaturated zone, a capillary fringe, a water table mound, a river cell and adjacent cells.

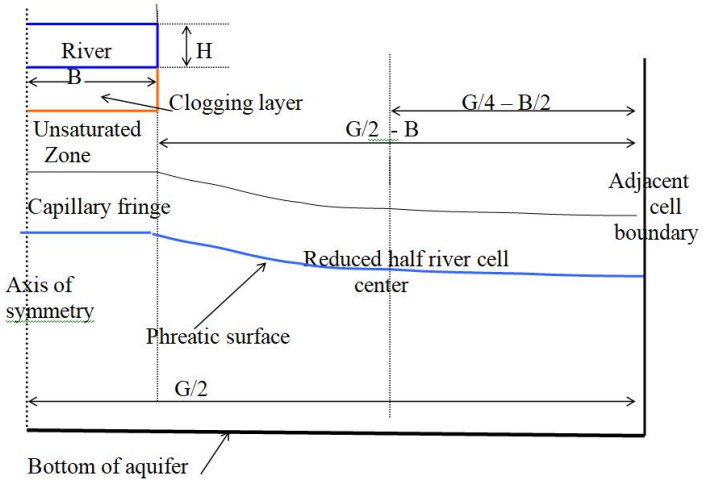

Fig. 2. Schematic view of the different components of system

Not only is the river cell divided into two halves but in addition the initial half-cell is reduced by the half-width of the water-table mound, B. So for that reason it is referred to as the *reduced* half river cell. It may be important to recognize that once desaturation has started the head in the *reduced half river cell,* still denoted h_f, is no longer exactly the head in the full river cell, denoted h_{frc}. If the river width is small relative to the width of the (aquifer) river cell, which in large-scale regional studies is usually the case, then the two heads are essentially the same. If that is not the case a very minor change is needed. By law of averaging:

$$h_f = \frac{Gh_{frc} - 2Bz_{rf}}{G - 2B} \quad (2)$$

provides the correction). G is the grid size, B half the river bottom width and z_{rf} is the water table mound height measured from the aquifer layer bottom.

One main objective of the approach is to simplify the analysis of the unsaturated connection condition by approximating the shape of the water content profile in the unsaturated zone instead of solving numerically the unsaturated flow equation (e.g. Richards equation).

3. INCIPIENT DESATURATION

When a river is in saturated connection with the underlying aquifer what could cause desaturation to occur? For that to happen the head in the aquifer cell that contains the river (the river cell) must drop significantly so that the flow between the river and the half river cell, under such a large driving head drop, cannot be maintained by the river unless there is a significant suction coming from the aquifer.

Desaturation in the aquifer will start when the suction at the bottom of the clogging layer, also the top of the aquifer, will be equal to the entry capillary pressure in drainage for the geologic material that makes the aquifer, h_{ce}.

(Throughout this article when the term “capillary pressure” is used, for brevity, it actually means capillary pressure “expressed as an equivalent water height” and has dimension of length).

That will cause *incipient* desaturation (incip). That value of head is obtained from the expression [5]:

$$h_f^{incip} = h_S - \frac{(B+H)K_{rcl}}{K_H \Gamma} \frac{(H + h_{ce} + e_{rcl})}{e_{rcl}} \quad (3)$$

h_S is the head in the stream, H is the river stage , K_{rcl} is the conductivity of the (real) clogging layer and e_{rcl} is its thickness In this formula Γ is the conductance that includes the possibility of anisotropy, of an excess far distance due to grid size and naturally the presence of the clogging layer [4].

We note that incipient desaturation will also depend upon the river head, the size of the wetted perimeter and naturally depends upon Γ, the one-sided stream-aquifer flow exchange (SAFE) dimensionless conductivity [5].

4. THE APPROXIMATE PROFILE OF THE UNSATURATED ZONE

The word *interface* refers to the boundary between the bottom of the clogging layer and the top of the underlying aquifer. We use the term *capillary zone* for the combination of both the *unsaturated zone* and the *capillary fringe*. Fig. 3 illustrates the water content profile shape under the river and the notations used in the unsaturated zone and the water table mound.

θ_I is the water content at the interface, θ is the **average** water content in the unsaturated zone and θ_S is the saturated water content. z_f is the depth of the unsaturated zone between the bottom of the clogging layer and the top of the capillary zone while z_{rf} is the elevation of the phreatic surface within the mound from the bottom of the aquifer.

Under an unsaturated connection if we knew the capillary pressure at the interface, h_{cI}, then we would know the seepage velocity at the interface, i_S,

given by Darcy’s law: $$i_S = K_{rcl} \frac{(H + h_{cI} + e_{rcl})}{e_{rcl}} \quad (4)$$

At the depth z_f the capillary pressure is known h_{ce}. What would be a reasonable capillary pressure (or equivalently water content or relative permeability) profile in between?

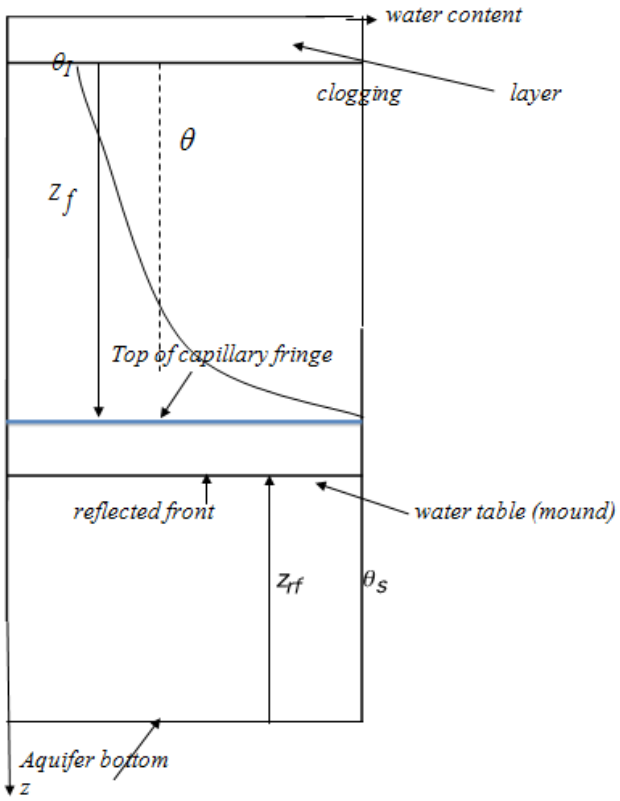

Fig. 3. Water content profile below the river

The flow rate at the bottom of the riverbed is the *seepage* rate. At the top of the capillary fringe the flow rate is the *recharge* rate to the aquifer. In MODFLOW, for example, no distinction is made between seepage and recharge rates. They are automatically deemed the same. That would be true under a steady-state condition. As an approximation it would seem reasonable (1) to use a steady-state profile associated with the seepage rate (or the recharge rate or a combination) and (2) to use a succession of steady-states to describe the transient behavior. Two procedures have been tried and the main purpose of this paper is to see how they compare.

4.1 First Choice for the Steady-state Profile in the Unsaturated Zone

This was a first approximation that was used and it may not be the most practical. Using a few additional assumptions regarding the Brooks-Corey parameters associated with the geologic material of the aquifer, namely M=2.5 and p=5 (M is the exponent in the expression of capillary pressure and p in the expression of relative conductivity, as power functions of normalized water content) such a profile is derived (for details see Appendix 2).

$$h_c^* = \frac{1 + h_{cI}^* \sqrt{v^*} - e^{D_z z^*}(1 - h_{cI}^* \sqrt{v^*})}{\sqrt{v^*}[1 + h_{cI}^* \sqrt{v^*} + e^{D_z z^*}(1 - h_{cI}^* \sqrt{v^*})]} \quad (5)$$

with $h_c^* = \frac{h_c}{h_{ce}}$ (6a) $z^* = \frac{z}{z_f}$ (6b) $v^* = \frac{v}{K_V}$ (6c)

$$D_z = \ln\{(\frac{1 + h_{cI}^* \sqrt{v^*}}{1 + \sqrt{v^*}})(\frac{1 - \sqrt{v^*}}{1 - h_{cI}^* \sqrt{v^*}})\} \quad (6d)$$

and $$z_f = \frac{h_{ce}}{2\sqrt{v^*}} \ln\{(\frac{1 + h_{cI}^* \sqrt{v^*}}{1 + \sqrt{v^*}})(\frac{1 - \sqrt{v^*}}{1 - h_{cI}^* \sqrt{v^*}})\} \quad (7)$$

v is the steady-state water velocity (in the Darcy sense) in the unsaturated zone. Having calculated h_c^* the normalized water content is obtained, θ^*,

since: $\theta^* = (h_c^*)^{-\frac{1}{M}}$ (8)

Having calculated the *point* values of water content along the profile in the unsaturated zone then one calculates the *average* value in that zone, θ. This is done by numerical integration in this case. This value will be used to estimate how much water has drained from the unsaturated zone during a period of time, $\Delta t = t - t^o$.

In these equations the steady-state velocity, v, is selected to be the seepage rate at the end of the period, i_S. The time at the beginning of the period of time is denoted t^o and at the end t^v (or simply t).

The recharge rate is the seepage rate plus the amount of water that has drained from the unsaturated zone into the capillary fringe in other words into the aquifer. The volume of water drained between the time t^o and the time t, the duration Δt, is the amount of air gained in that zone in other words is:

$$\Delta V_{drain} = \frac{(\theta_S - \theta) z_f}{\Delta t} - \frac{(\theta_S - \theta^o) z_f^o}{\Delta t} \quad (9)$$

If indeed there is drainage, because the water-table is receding, both $\theta \le \theta^o$ and $z_f \ge z_f^o$ and ΔV_{drain} is positive. It is the reverse if the water-table is rising.

In this equation θ refers to the average water content within the unsaturated zone. The recharge rate by mass balance is thus:

$$v_{rech}^{mass} = i_S + \frac{(\theta_S - \theta) z_f}{\Delta t} - \frac{(\theta_S - \theta^o) z_f^o}{\Delta t} \quad (10)$$

(Even though the numerical value of *Δt* is 1 (say a day), as a check on proper dimensionality of the derived expressions it is better to keep it explicitly. The superscript "mass" is not generally shown when mass estimate is meant). The superscript "o" refers to *old* values, at the beginning of a period (time step). The superscript "v" (or no superscript) refers to *new* values, at the end of the period.

4.2 Second Choice for the Steady-state Profile in the Unsaturated Zone

In this case a different functional relationship is assumed between relative permeability and capillary pressure namely: $k_{rw} = e^{-\frac{(h_c - h_{ce})}{H_{cS}}}$ (11)

Using this formulation (Appendix 1) one obtains:

$$(k_{rw})_{mean} = v^* + \frac{[1 - k_{rw}(h_{cI})]}{\ln[\frac{1 - v^*}{k_{rw}(h_{cI}) - v^*}]} \quad (12)$$

$$(h_c)_{mean} = h_{ce} - H_{cS} \ln[(k_{rw})_{mean}] \quad (13)$$

$$\theta = \theta_{mean} = \theta_r + (\theta_S - \theta_r)[\frac{(h_c)_{mean}}{h_{ce}}]^{-\frac{1}{M}} \quad (14)$$

$$z_f = H_{cS} \ln[\frac{1 - v^*}{k_{rw}(h_{cI}) - v^*}] \quad (15)$$

Eqs.(9) and (10) still apply.

5. THE THICKNESS OF THE UNSATURATED ZONE, z_f

Even though a value can be obtained from the steady-state profile a more dynamic approach is used. The details of the derivations are available in an earlier article [6] and only a summary is provided.

$C_{ap}R_{es}$ is the capillary resistance, a negative value defined as:

$$C_{ap}R_{es} = -H_{cS}[1-(h_{cI}^{*})^{-\frac{p-M}{M}}] \tag{16}$$

The instantaneous recharge rate is

$$v_{rech}^{dyn} = 2K_V[\frac{C_{ap}R_{es}}{z_f} + k_{rw}(\theta)] - i_S \tag{17}$$

Eq.(10) is a mass estimate of the recharge rate. We then require that the two estimates given by Eqs.(10) and (17) yield the same estimate of z_f, mathematically a second order algebraic equation:

$$i_S + [\frac{(\theta_S - \theta)z_f}{\Delta t} - \frac{(\theta_S - \theta^o)z_f^o}{\Delta t}] = 2K_V[\frac{C_{ap}R_{es}}{z_f} + k_{rw}(\theta)] - i_S \tag{18}$$

The solution of that algebraic second order equation yields the value of z_f.

6. THE ELEVATION OF THE WATER-TABLE MOUND, z_{rf}

The water table mound is excited by the recharge rate from the river and the lateral outflow to (or inflow from) the part of the river cell which is not below the river. Mass balance for the position of the mound is:

$$\begin{aligned}\phi_{ef}(B+H)\frac{dz_{rf}}{dt} &= (B+H)v_{rech} - \Gamma K_H(z_{rf} - h_f) \\ &= (B+H)\{2K_V[\frac{C_{ap}R_{es}}{z_f} + k_{rw}] - i_S\} - \Gamma K_H(z_{rf} - h_f)\end{aligned} \tag{19}$$

In this expression ϕ_{ef} is the specific yield (effective porosity) in the mound region. The SAFE dimensionless conductance appearing in Eq. (19) is $\Gamma_{flat-anis-\Delta}$ accounting for the fact that there is no longer river penetration, the possibility of anisotropy in the aquifer and an excess distance from the standard far distance [4].

The solution (for details see Appendix 3) for $z_{rf}(n)$ (where n is the period (usually day) number for time) is:

$$z_{rf}(n) = \rho_{rf} z_{rf}(n-1) + \alpha_{rf}[h_f(n-1) + \sigma_{rf} v_{rech}(n-1)]$$

$$+\beta_{rf}[h_f(n) + \sigma_{rf} v_{rech}(n)] \quad (20)$$

$$\rho_{rf} = e^{-\frac{1}{C_{rf}}} \quad (21a) \quad \alpha_{rf} = [C_{rf}(1-\rho_{rf}) - \rho_{rf}] \quad (21b) \quad \beta_{rf} = [1 - C_{rf}(1-\rho_{rf})] \quad (21c)$$

This is the *dynamic* estimate for z_{rf} so z_{rf}^{dyn}. But by mass balance it can be estimated as $z_{rf}^{mass} = z_{rf} = D - e_{rcl} - z_f - h_{ce}$ (22). Naturally the two values should be the same. D is the distance from the river bottom to the aquifer bottom.

7. PROCEDURAL STEPS IN CASE OF DESATURATION

The external excitations to the system are the stage (maximum water depth) in the river, *H*, and the head in the part of the half river cell away from the banks, h_f. The first step is to estimate (guess) the value of the interface capillary pressure, h_{cI}, and thus determine θ_I, θ and i_S as well. Then one estimates a value for z_f by requiring that the recharge rates estimated by mass balance and dynamically be the same, using Eq. (18). That defines a value of z_f. Next the value of z_{rf} is obtained by mass balance and dynamically.

One estimates the value of z_{rf} using Eq.(22) and dynamically, z_{rf}^{dyn}, using Eq. (20).

Had one chosen the right value for h_{cI} the two estimated values for z_{rf} would be the same. If they are not the same then iteratively one chooses other values of h_{cI} so that ultimately the two values match within a given tolerance. Once that tolerance is met the right values of h_{cI} and of all the other variables were obtained. The numerical algorithm guarantees that mass balance is always secured.

8. COMPARISON OF THE TWO UNSATURATED ZONE METHODS

The basic parameters for the comparison are in Table 1.

Saturated water content = 0.4; residual water content = 0.2

Table 1. Parameters of the system

Parameter	Definition	Unit	Value
D	Aquifer thickness below river bottom	m	20
B	Half-width of the river	m	5
G	Lateral grid	m	200
K_H	Aquifer hydraulic conductivity (horizontal)	m/day	2.5
K_V	Aquifer hydraulic conductivity (vertical)	m/day	2.5
K_{rcl}	Hydraulic conductivity of clogging layer	m/day	0.01
e_{rcl}	Thicknesss of clogging layer	m	0.4
h_{ce}	BC air entry value, aquifer	m	0.30
	BC air entry value, clogging layer	m	2.00
M	BC exponent, aquifer	-	2.5
	BC exponent, clogging layer	-	2.5
p	BC Exponent conductivity aquifer	-	5
	BC exponent conductivity clogging layer	-	5
H	Water level in river (river stage)	m	0.1
ϕ_e	Aquifer effective porosity		0.2
h_f^{ini}	Initial head in reduced half river cell	m	20.7

Fig. 4 shows the comparison for the capillary pressure at the interface.

If the value exceeds 0.30 m then the connection is unsaturated. Otherwise it is saturated. The simulation starts with the system under saturated connection.

Naturally when in a saturated connection the results are identical since the same methodology applies. That changes at time 8. The system remains in unsaturated connection till time 36 where it changes again to a saturated connection. Now during that period and later there is a slight difference between methods 1 and 2 for the unsaturated connection. However the differences are minor.

Fig. 5 shows the comparison for the seepage rates. These are the important variables. The same conclusions hold.

Fig. 6 shows the comparison for the recharge rates. The same conclusions hold. The difference are minor.

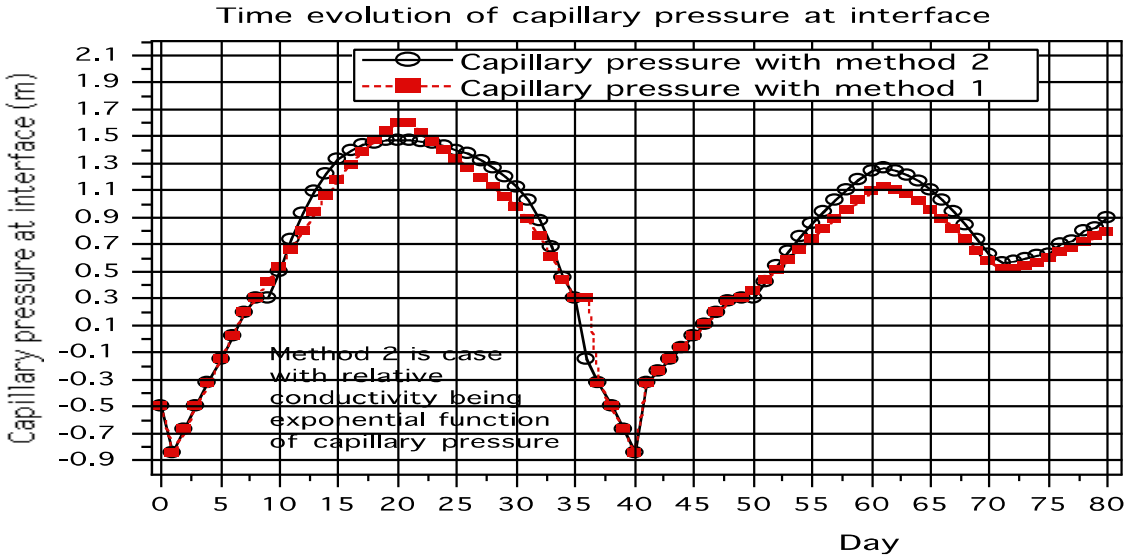

Fig. 4. Comparison for the capillary pressure at the interface

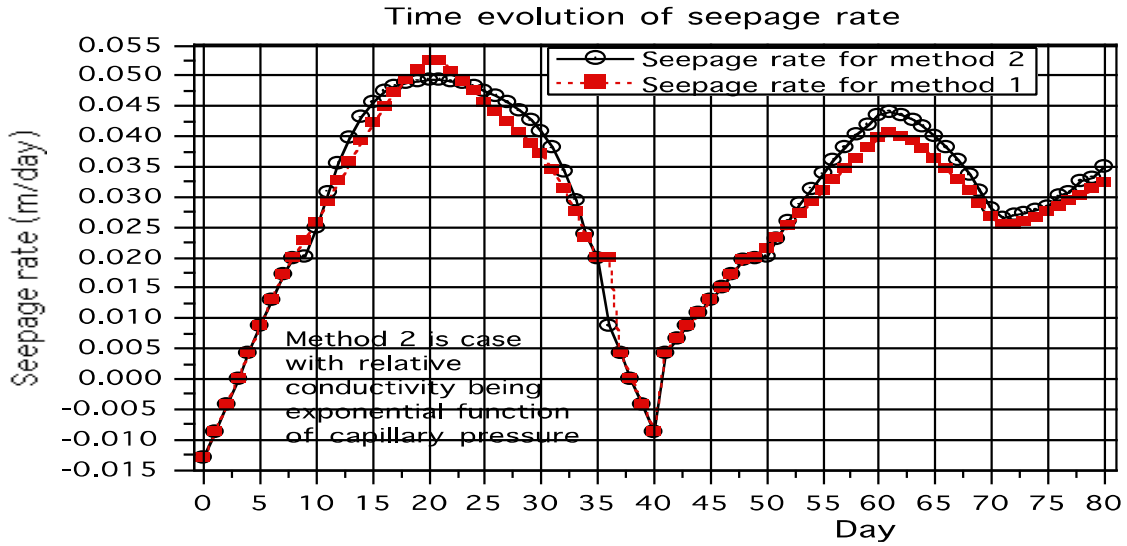

Fig. 5. Comparison for the seepage rates

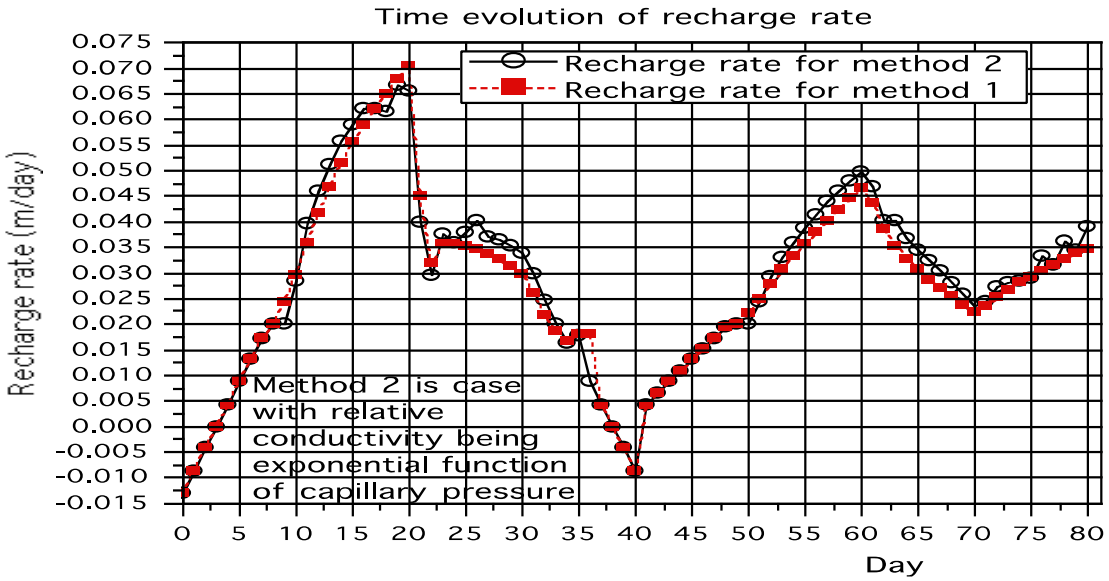

Fig. 6. Comparison for the recharge rates

Note that with these approaches the seepage and recharge rates are not the same and in reality they are not. In models like MODFLOW they are assumed to be the same. As the water-table draws down the drainage from the unsaturated zone is added to the seepage rate to constitute the recharge rate. Vice versa when the water-table rises some of the upward inflow replenishes the unsaturated zone and the seepage rate is higher than the recharge rate.

The difference between seepage and recharge rates is shown in Fig. 7 for model 1.

Fig. 8 shows the difference between seepage and recharge rates for model 2. The patterns are similar for the two models.

Finally Fig. 9 shows the pattern of evolution of the head in the (reduced half) river cell. Incipient desaturation happens for the value of head = 19.1749 m. The same value characterizes incipient resaturation because in this simulation the river stage keeps the same value throughout. From time 20 to 21 there is a significant increase in the head, leading to significant changes in values of seepage and recharge as can be seen in Figs. 5, 6, 7 and 8.

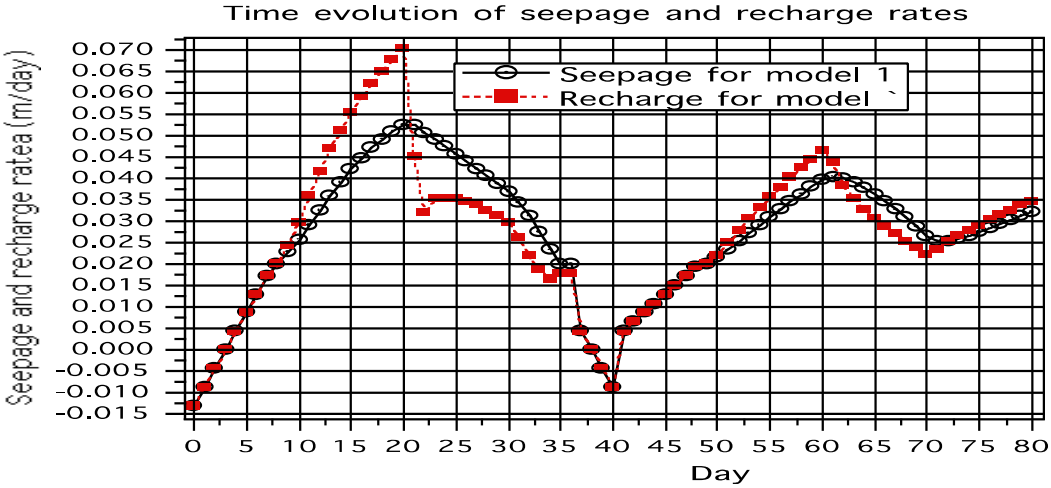

Fig. 7. Comparison of seepage and recharge rates for model 1

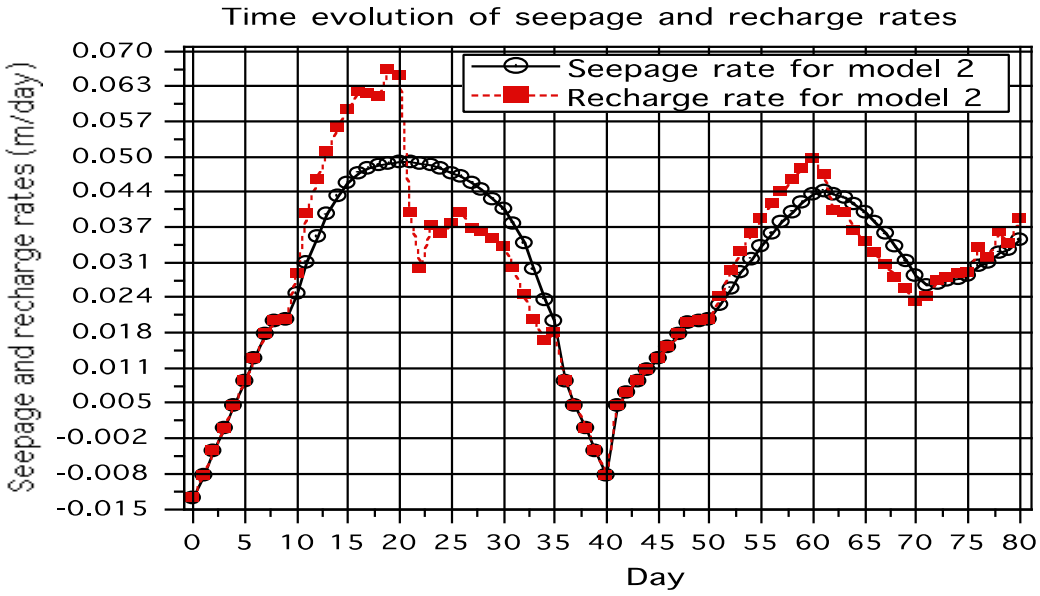

Fig. 8. Comparison of seepage and recharge rates for model 2

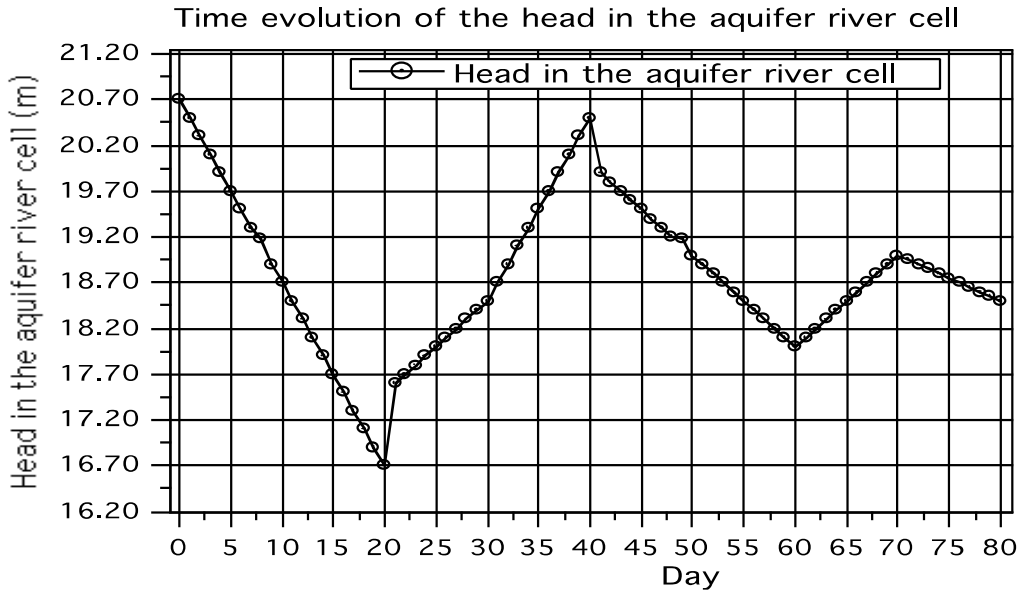

Fig. 9. Pattern of evolution of head in the (reduced half) river cell

9. DISCUSSION

The main purpose of this article was to compare the two models developed to describe the unsaturated zone when the connection between the river and the aquifer is unsaturated. First the two models had to be described in some details.

In real situations the determination of seepage and recharge would be dependent upon river stage and heads further away from the river cell. These cells would be conditioned by the overall aquifer system behavior in a large region. Thus that head should at least the head in an adjacent cell, h_{adj}. Using the head in the river cell as a boundary condition is not realistic when considering a complex regional situation. However in this article the focus was not on how this approach would be integrated into a full

regional hydrologic model but to test its capability to describe seepage and recharge. What drives the exchange flow between the stream and the aquifer is the fluctuating head drop between the river and the aquifer. Since it depends on that drop and not on the individual values of head in the river and in the aquifer river cell, it did not matter for this numerical example how that drop fluctuates as long as it does. This is why in this simulation the river stage could remain constant.

In real circumstances the river stage would not be a boundary condition. It would be a state variable conditioned by the surface river flow, characterized by a routing model. How to proceed for real situations has been suggested in other articles and most recently [6,7]. The two models discussed for description of the unsaturated zone turned have produced fortunately very similar results. That in no way proves that they are accurate or at least accurate enough. To prove that acceptable accuracy, a similar study would have to be conducted using a two-dimensional simulation using a numerical solution of Richards equation.

However since full solution of Richards equation could not be practically included in codes for large-scale regional studies one has to be satisfied with an improvement over the very crude approach currently in use. The fact, for example, that the new approach is able to distinguish between seepage and recharge, whereas in MODFLOW they are systematically assumed to be the same, is already an indication of its superiority, at least in theory. In this simulation when the connection is unsaturated the head in the river cell is smaller than the elevation of the river bottom and that is true for all the times when the connection is unsaturated. Thus MODFLOW would calculate a constant seepage rate according to the formula [3]:

$$i_S = \frac{K_{rl}}{e_{rcl}}[h_S - h_{brb}] = \frac{K_{rl}}{e_{rcl}}[H + e_{rcl}] \qquad (23)$$

Numerically: $i_S = \frac{0.01}{0.4}[0.1 + 0.4] = 0.0125$ m/day.

Fig. 10 shows the differences for seepage calculated for models 1 and 2 and according to River Package (RP) [1].

The differences are major when the connection is unsaturated. In the simulation the leakance coefficient for the RP method is the leakance coefficient of the clogging layer that is $\Lambda_{rcl} = \frac{K_{rcl}}{e_{rcl}}$ (24). (In large-scale simulations for real systems that leakance coefficient would be calibrated). During the periods when the connection is saturated the difference

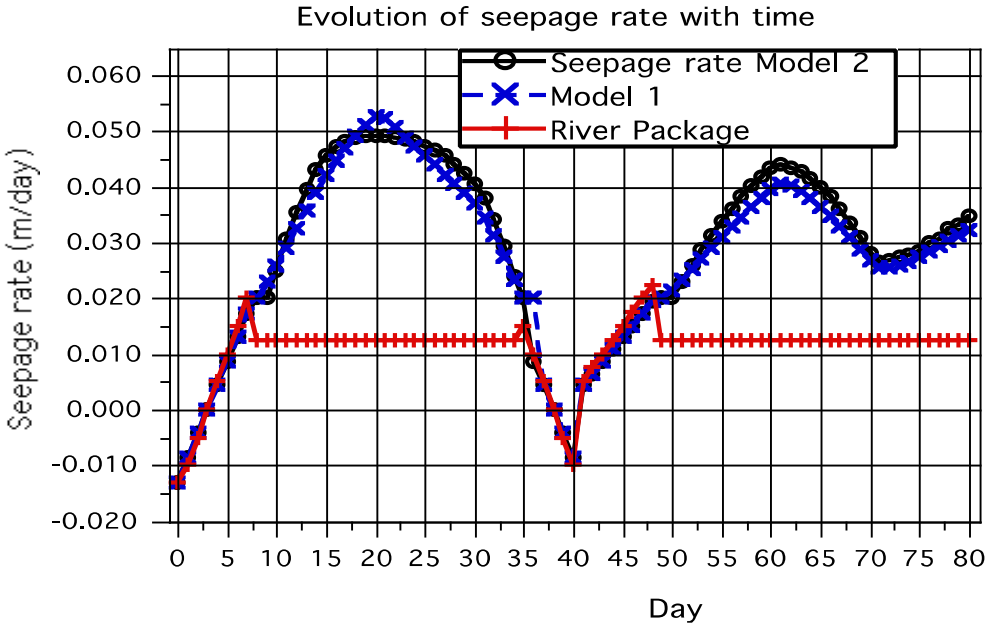

Fig. 10. Comparison of seepage results calculated by different methods

between the 3 approaches is very minor. However this is due primarily because the resistance in this simulation in the clogging layer is large and fully obscures the other resistances. Finally the seepage calculated by Models 1 and 2 is large because the suction exerted by the unsaturated zone is very large, rising up to 1.5 m as shown in Fig. 4. Such high suction is possible because the drainage entry pressure of the clogging layer is assumed to be 2 m as shown in Table 1. The clogging layer remains saturated. That assumption needs to be questioned. In practice it is doubtful that the riverbed would remain saturated so long when there is a large suction in the aquifer under the riverbed. The value of 2 meters may be unrealistic and thus the differences shown in Fig. 10 may be grossly exaggerated. A study of what realistic values can be for the riverbed depending its soil classification would be useful. A different analysis is required for an approximate solution when there is drainage occurring within the riverbed itself. That would definitely be the case when the river goes dry.

For the sake of completeness full results of the simulation runs for Models 1 and 2 are provided in Appendix 4.

10. CONCLUSIONS

Both models 1 and 2 estimate approximately a water content (or capillary pressure or relative conductivity) profile in the unsaturated zone beneath the riverbed and above the phreatic surface of the water-table aquifer. From that profile the seepage and the aquifer recharge rates are derived.

The difference between these two models is in the choice of the approximate profile. In model 1 the way the profile is chosen is somewhat more refined but it was derived for one set of parameters characterizing the soil type of the material of the aquifer, namely p and M. Only for a few other values of these parameters can a profile be derived exactly. On the other hand with the second model all values of these parameters can be used. This it is a more universal model.

The practical benefit of the comparison is that it is possible to use the simpler method, model 2, to describe the unsaturated zone behavior with essentially the same results obtained with the more numerically complicated and less general method, model 1. This is important because if inserted in large-scale numerical models the new methodology should not create a significant added numerical burden. After all, MODFLOW's approach to calculate seepage may be rather crude and violating basic physical principles but it has the advantage of not adding numerical work to a groundwater system already under numerical stress.

ACKNOWLEDGEMENTS

The SAFE methodology's successful development over many years was made possible by the cooperative and effective work of Calvin Miller, Steffen Mehl and Cinzia Miracapillo, as evident in the references list. Fig. 1 was provided by Cinzia Miracapillo. The sustained interest for the project of Tariq Kadir and Can Dogrul, both of the California Dept. of Water Resources, is greatly appreciated.

COMPETING INTERESTS

Author has declared that no competing interests exist.

REFERENCES

1. McDonald M, Harbaugh A. A modular three-dimensional finite-difference ground-water flow model: Techniques of water-resources investigations of the United States Geological Survey. Book 6, Chapter A1. 1988;586.
2. Morel-Seytoux HJ, Miller C, Mehl S, Miracapillo C. Achilles' heel of integrated hydrologic models: The stream-aquifer flow exchange and proposed alternative. Journal of Hydrology. 2018;564:900-908. Available:https://doi.org/10.1016/j.jhydrol.2018.07.010
3. Morel-Seytoux HJ. MODFLOW's River package: Part 1: A critique. Physical Science International Journal. 2019a;22(2): 1-9. Article no.PSIJ.49757 DOI: 10.9734/PSIJ/2019/v22i230129
4. Morel-Seytoux HJ, Calvin D. Miller, Cinzia Miracapillo, Steffen Mehl. River seepage conductance in large-scale regional studies. ©2016, National Ground Water Association; 2016. DOI: 10.1111/gwat.12491
5. Morel-Seytoux HJ. Two dimensional analytical derivation of incipient desaturation criterion in stream-aquifer

flow exchange. Journal of Geography, Environment and Earth Science. 2019d;23(4):1-14.

6. Morel-Seytoux HJ. MODFLOW's River package: Part 2: Correction, combining analytical and numerical approaches. Physical Science International Journal. 2019c;22(3):1-23. Article no.PSIJ.49758 DOI: 10.9734/PSIJ/2019/v22i330131

7. Morel-Seytoux HJ. Analytical River routing with alternative methods to estimate seepage. International Journal of Environment and Climate Change. 2019b;9(3):167-192. DOI: 10.9734/IJECC/2019/V9I330106

Appendix 1. Steady-state unsaturated zone water content profile assuming relative permeability to be an exponential function of capillary pressure

Nevertheless still assuming the B-C relation between water content and capillary pressure holds.

Darcy's velocity equation is:

$$v_w = K_V k_{rw}[\frac{\partial h_c}{\partial z} + 1] \tag{1}$$

with the vertical coordinate z oriented positive downward with origin at the bottom of the clogging layer. It is convenient to define a normalized capillary pressure and normalized vertical coordinate:

$$h_c^* = \frac{h_c}{h_{ce}} \tag{2}$$

$$z^* = \frac{z}{z_f} \tag{3}$$

where z_f is the depth of the unsaturated zone above the capillary fringe.

In terms of capillary pressure and coordinate z the velocity is:

$$v_w = K_V[k_{rw}\frac{\partial h_c}{\partial z} + k_{rw}] \tag{4}$$

Mass conservation under steady-state is: $\frac{\partial v_w}{\partial z} = 0$ or $v_w = \text{constant}$ (5)

Define the capillary drive in the form:

$$H_c(h_c) = \int_{h_{ce}}^{h_c} k_{rw}(\eta_c)d\eta_c \tag{6}$$

and thus: $\frac{\partial H_c(h_c)}{\partial z} = k_{rw}(h_c)\frac{\partial h_c}{\partial z}$ (7)

which transforms the velocity expression as:

$$v_w = K_V[\frac{\partial H_c}{\partial z} + k_{rw}] \tag{8}$$

Steady-state requires: $\frac{\partial H_c(h_c)}{\partial z} + k_{rw}(h_c) = v^*$ (9)

Now assume an exponential variation of the relative conductivity as a function of capillary pressure:

$$k_{rw} = e^{-\alpha(h_c - h_{ce})} = (e^{\alpha h_{ce}})e^{-\alpha h_c} \quad (10)$$

Substitution in Eq.(6) yields:

$$H_c(h_c) = \int_{h_{ce}}^{h_c} (e^{\alpha h_{ce}})e^{-\alpha x}dx = e^{\alpha h_{ce}}(\frac{-1}{\alpha})e^{-\alpha x}\Big|_{h_{ce}}^{h_c} = (\frac{1}{\alpha})[1 - e^{-\alpha(h_c - h_{ce})}] = \frac{1 - k_{rw}}{\alpha} \quad (11)$$

Given that $H_c(\infty) = \int_{h_{ce}}^{\infty} k_{rw}(\eta_c)d\eta_c = H_{cS} = \frac{Mh_{ce}}{p - M}$ (12)

It follows that:

$\frac{1}{\alpha} = H_{cS}$ (13) $k_{rw} = e^{-\frac{(h_c - h_{ce})}{H_{cS}}}$ (14) $H_c(h_c) = H_{cS}[1 - k_{rw}(h_c)]$ (15)

It follows that $\frac{\partial H_c(h_c)}{\partial z} = -H_{cS}\frac{\partial k_{rw}(h_c)}{\partial z}$ (16)

Substitution in Eq.(9): $k_{rw}(h_c) - H_{cS}\frac{\partial k_{rw}(h_c)}{\partial z} = v^*$ (17)

Solution is of the form: $k_{rw}(h_c) = Ae^{\beta z} + D$. Substitution yields:

$$Ae^{\beta z} + D - H_{cS}A\beta e^{\beta z} = v^* \text{ or } k_{rw}(h_c) = Ae^{\frac{z}{H_{cS}}} + v^* \quad (18)$$

Boundary conditions are that for $h_c = h_{ce}$ when $z = z_f$ $k_{rw} = 1$ so

$$1 - v^* = Ae^{\frac{z_f}{H_{cS}}} \quad (19)$$

and at the bottom of the clogging layer $z = 0$ and $h_c = h_{cI}$

thus $k_{rw}(h_{cI}) = A + v^*$ and $A = k_{rw}(h_{cI}) - v^*$

Substitution in Eq.(19): $1 - v^* = [k_{rw}(h_{cI}) - v^*]e^{\frac{z_f}{H_{cS}}}$ $z_f = H_{cS}\ln[\frac{1 - v^*}{k_{rw}(h_{cI}) - v^*}]$ (20)

{Note that for this equation to have meaning the argument of the logarithm must be positive. Typically the normalized seepage rate $v^* = \frac{v}{K_V} = \frac{K_{rcl}}{K_V}[\frac{H + h_{cI} + e_{rcl}}{e_{rcl}}]$ is less than 1 which then requires that

$$1 \geq k_{rw}(h_{cI}) \geq v^*$$

At incipient desaturation when $h_{cI} = h_{ce}$ when $v^* \leq 1$ then $k_{rw}(h_{cI}) = 1$

As h_{cI} gradually increases v^* increases but $k_{rw}(h_{cI})$ decreases so that z_f eventually would approach infinity, which never happens practically because that would require that the water-table had dropped tremendously}

Finally: $k_{rw}(h_c) = [k_{rw}(h_{cI}) - v^*]e^{\frac{z_f}{H_{cS}}z^*} + v^*$ (21)

One can calculate the average value of the relative permeability over the unsaturated zone:

$$(k_{rw})_{mean} = \int_0^1 \{[k_{rw}(h_{cI}) - v^*]e^{\frac{z_f}{H_{cS}}z^*} + v^*\}dz^* \quad (22)$$

$$(k_{rw})_{mean} = v^* + [k_{rw}(h_{cI}) - v^*]\frac{H_{cS}}{z_f}(e^{\frac{z_f}{H_{cS}}} - 1)$$

$$= v^* + \frac{H_{cS}}{z_f}[1 - k_{rw}(h_{cI})] \quad = v^* + \frac{1 - k_{rw}(h_{cI})}{\ln[\frac{1 - v^*}{k_{rw}(h_{cI}) - v^*}]} \quad (23)$$

Then assuming that the average capillary pressure is the capillary pressure associated with the average relative conductivity then:

$$(h_c)_{mean} = h_{ce} - H_{cS}\ln[(k_{rw})_{mean}] \quad (24)$$

Since the argument of the logarithm is less than one the value of the left hand side, $(h_c)_{mean}$, is greater than h_{ce} as it should be.

Similarly: $(\theta^*)_{mean} = [\frac{(h_c)_{mean}}{h_{ce}}]^{-\frac{1}{M}}$; $\theta_{mean} = \theta_r + (\theta_S - \theta_r)(\theta^*)_{mean}$ (25)

Appendix 2. "Steady-state unsaturated seepage water content profile assuming Brooks-Corey functions"

Darcy's equation for velocity : $$v^* = \frac{v}{K_V} = k_{rw}[\frac{h_{ce} dh_c^*}{dz} + 1] \quad (1)$$

Expressing k_{rw} as a function of h_c:

$$k_{rw} = (h_c^*)^{-\frac{p}{M}} = (h_c^*)^{-\alpha} \quad (2)$$

Substitution in Eq. (1) yields:

$$v^* = (h_c^*)^{-\alpha}[\frac{h_{ce} dh_c^*}{dz} + 1] \quad \text{or} \quad \frac{v^* - (h_c^*)^{-\alpha}}{(h_c^*)^{-\alpha}} = \frac{h_{ce} dh_c^*}{dz} \quad (3)$$

Separation of variables yields:

$$\frac{(h_c^*)^{-\alpha} dh_c^*}{v^* - (h_c^*)^{-\alpha}} = \frac{dz}{h_{ce}} \quad (4)$$

Let $x = h_c^* \sqrt{v^*}$ then $h_c^* = x / \sqrt{v^*}$ and $dh_c^* = \frac{dx}{\sqrt{v^*}}$

Substitution in Eq. (4) yields:

$$\frac{(\frac{x}{\sqrt{v^*}})^{-\alpha} \frac{dx}{\sqrt{v^*}}}{v^* - (\frac{x}{\sqrt{v^*}})^{-\alpha}} = \frac{dz}{h_{ce}} \quad (5)$$

In case $\alpha = 2$

$$\frac{(\frac{v^*}{x^2}) \frac{dx}{\sqrt{v^*}}}{v^* - \frac{v^*}{x^2}} = \frac{dz}{h_{ce}} \quad \text{or} \quad \frac{\frac{dx}{\sqrt{v^*}}}{x^2 - \frac{1}{x^2}} = \frac{dz}{h_{ce}} \quad \text{or} \quad \frac{dx}{1 - x^2} = -\sqrt{v^*} \frac{dz}{h_{ce}} \quad (6)$$

Note that Eq. (4) is also integrable exactly for values of α equal to 3 and 4. Integration of Eq. (5b) between the limits $h_c^* \sqrt{v^*}$ and $h_{cI}^* \sqrt{v^*}$ yields:

$$\frac{1}{2}\ln(\frac{1+x}{1-x})\Big|_{h_c^*\sqrt{v^*}}^{h_{cI}^*\sqrt{v^*}} = \frac{\sqrt{v^*}z}{h_{ce}} \tag{7}$$

or ultimately:

$$\frac{1}{2}\ln\{(\frac{1+h_{cI}^*\sqrt{v^*}}{1+h_c^*\sqrt{v^*}})(\frac{1-h_c^*\sqrt{v^*}}{1-h_{cI}^*\sqrt{v^*}})\} = \frac{\sqrt{v^*}}{h_{ce}}z \tag{8}$$

When $h_c^* = 1$, one is at the top of the capillary fringe and then:

$$\frac{1}{2}\ln\{(\frac{1+h_{cI}^*\sqrt{v^*}}{1+\sqrt{v^*}})(\frac{1-\sqrt{v^*}}{1-h_{cI}^*\sqrt{v^*}})\} = \frac{\sqrt{v^*}}{h_{ce}}z_f \tag{9}$$

Defining: $$D_z = \ln\{(\frac{1+h_{cI}^*\sqrt{v^*}}{1+\sqrt{v^*}})(\frac{1-\sqrt{v^*}}{1-h_{cI}^*\sqrt{v^*}})\} \tag{10}$$

and dividing Eq.(8) by Eq.(9) one obtains:

$$z^* = \frac{z}{z_f} = \ln\{(\frac{1+h_{cI}^*\sqrt{v^*}}{1+h_c^*\sqrt{v^*}})(\frac{1-h_c^*\sqrt{v^*}}{1-h_{cI}^*\sqrt{v^*}})\} / D_z \tag{11}$$

which solved for the normalized capillary pressure yields:

$$h_c^* = \frac{1+h_{cI}^*\sqrt{v^*} - e^{D_z z^*}(1-h_{cI}^*\sqrt{v^*})}{\sqrt{v^*}[1+h_{cI}^*\sqrt{v^*} + e^{D_z z^*}(1-h_{cI}^*\sqrt{v^*})]} \tag{12}$$

One can verify that for $z^* = 0$ one obtains correctly $h_c^* = h_{cI}^*$. For $z^* = 1$ one obtains also correctly $h_c^* = 1$. That follows from the very definition of the parameter D_z.

If $v^* < 0$ let $\tan(h_{cI}^*\sqrt{-v^*}) = A$, $\tan(\sqrt{-v^*}) = P$ and $D_z = A - P$

The relation between normalized capillary pressure and normalized unsaturated zone coordinate $z^* = \frac{z}{z_f}$ is:

$$z^* = \frac{A - \tan(h_c^* \sqrt{-v^*})}{D_z} \text{ or } h_c^* = \frac{\tan^{-1}[A - D_z z^*]}{\sqrt{-v^*}}$$

while the full thickness of the unsaturated zone is: $z_f = \frac{h_{ce} D_z}{\sqrt{-v^*}}$

Appendix 3. "Constant C Linear Reservoir type equation with a right hand-side excitation varying linearly with time

The excitation varies linearly in time and thus the basic governing equation is:

$$C\frac{dU}{dt} + U = E_o + (E_v - E_o)t \tag{1}$$

We look for a solution of the form: $U(t) = A + Mt + De^{-\frac{t}{C}}$ (2)

$$\frac{dU(t)}{dt} = M - \frac{D}{C}e^{-\frac{t}{C}} \tag{3}$$

Substitution in Eq. (1) yields:

$$C(M - \frac{D}{C}e^{-\frac{t}{C}}) + [A + Mt + De^{-\frac{t}{C}}] = E_o + (E_v - E_o)t \tag{4}$$

Satisfaction of the equation requires that:

$$M = (E_v - E_o) \tag{5}$$

and

$$A = E_o - C(E_v - E_o) \tag{6}$$

Substitution in Eq. (2) yields:

$$U(t) = E_o - C(E_v - E_o) + (E_v - E_o)t + De^{-\frac{t}{C}} \tag{7}$$

At time zero then: $U(0) = E_o - C(E_v - E_o) + D$ (8)

which yields D.

Substitution in Eq. (7) yields:

$$U(t) = U(0)e^{-\frac{t}{C}} + [E_o - C(E_v - E_o)](1 - e^{-\frac{t}{C}}) + (E_v - E_o)t \tag{9}$$

Application for end of period n making $t = 1$ and setting $\rho_U = e^{-\frac{1}{C}}$ (10)

yields:

$$U(n) = \rho_U U(n-1) + (1-\rho_U)\{E(n-1) - C[E(n) - E(n-1)]\} + [E(n) - E(n-1)] \quad (11)$$

Grouping terms:

$$U(n) = \rho_U U(n-1) + \{(1-\rho_U)(1+C) - 1\}E(n-1) + \{1 - C(1-\rho_U)\}E(n) \quad (12)$$

or

$$U(n) = \rho_U U(n-1) + [C(1-\rho_U) - \rho_U]E(n-1) + [1 - C(1-\rho_U)]E(n) \quad (13)$$

with $\alpha_U = [C(1-\rho_U) - \rho_U]$ (14a)

$$\beta_U = [1 - C_U(1-\rho_U)] \quad (14b)$$

then Eq.(13) becomes: $U(n) = \rho_U U(n-1) + \alpha_U E(n-1) + \beta_U E(n)$ (15)

Appendix 4. Tabulated full results of the simulation for Models 1 and 2

Simulation results for Model 1 -- unsatseep#22_results_2018.mp

DAY	JUNSAT	HCI	ZF	HSTAGE	ZRF	HF	HFRP	AISRP	AIS	VRECH	WCI	WC
0	-1	-0.5000	0.0000	20.1000	20.0000	20.7000	20.7000	-.0130	-.0130	-.0130	0.4000	0.4000
1	-1	-0.8477	0.0000	20.1000	20.4584	20.5000	20.5000	-.0100	-.0087	-.0087	0.4000	0.4000
2	-1	-0.6737	0.0000	20.1000	20.2790	20.3000	20.3000	-.0050	-.0043	-.0043	0.4000	0.4000
3	-1	-0.5000	0.0000	20.1000	20.1000	20.1000	20.1000	0.0000	0.0000	0.0000	0.4000	0.4000
4	-1	-0.3265	0.0000	20.1000	19.9214	19.9000	19.9000	0.0050	0.0043	0.0043	0.4000	0.4000
5	-1	-0.1533	0.0000	20.1000	19.7431	19.7000	19.7000	0.0100	0.0087	0.0087	0.4000	0.4000
6	-1	0.0197	0.0000	20.1000	19.5653	19.5000	19.5000	0.0150	0.0130	0.0130	0.4000	0.4000
7	-1	0.1923	0.0000	20.1000	19.3878	19.3000	19.3000	0.0200	0.0173	0.0173	0.4000	0.4000
8	1	0.3000	0.0000	20.1000	19.2774	19.1749	19.2169	0.0125	0.0200	0.0200	0.4000	0.4000
9	1	0.4177	0.1193	20.1000	19.1807	18.9000	18.9143	0.0125	0.0229	0.0245	0.3752	0.3866
10	1	0.5306	0.2357	20.1000	19.0643	18.7000	18.7186	0.0125	0.0258	0.0296	0.3592	0.3768
11	1	0.6644	0.3777	20.1000	18.9223	18.5000	18.5215	0.0125	0.0291	0.0359	0.3455	0.3676
12	1	0.8019	0.5302	20.1000	18.7698	18.3000	18.3240	0.0125	0.0325	0.0416	0.3350	0.3597
13	1	0.9366	0.6891	20.1000	18.6109	18.1000	18.1261	0.0125	0.0359	0.0468	0.3268	0.3532
14	1	1.0643	0.8523	20.1000	18.4477	17.9000	17.9279	0.0125	0.0391	0.0514	0.3205	0.3477
15	1	1.1822	1.0187	20.1000	18.2813	17.7000	17.7296	0.0125	0.0421	0.0555	0.3156	0.3430
16	1	1.2887	1.1876	20.1000	18.1124	17.5000	17.5312	0.0125	0.0447	0.0591	0.3116	0.3390
17	1	1.3833	1.3591	20.1000	17.9409	17.3000	17.3327	0.0125	0.0471	0.0622	0.3085	0.3356
18	1	1.4667	1.5343	20.1000	17.7657	17.1000	17.1340	0.0125	0.0492	0.0651	0.3060	0.3326
19	1	1.5404	1.7172	20.1000	17.5828	16.9000	16.9348	0.0125	0.0510	0.0680	0.3040	0.3299
20	1	1.6046	1.9072	20.1000	17.3928	16.7000	16.7353	0.0125	0.0526	0.0705	0.3023	0.3275
21	1	1.5971	1.8126	20.1000	17.4874	17.6000	17.5943	0.0125	0.0524	0.0451	0.3025	0.3278
22	1	1.5293	1.6073	20.1000	17.6927	17.7000	17.6996	0.0125	0.0507	0.0318	0.3043	0.3303
23	1	1.4609	1.4664	20.1000	17.8336	17.8000	17.8017	0.0125	0.0490	0.0355	0.3062	0.3328
24	1	1.3941	1.3378	20.1000	17.9622	17.9000	17.9032	0.0125	0.0474	0.0355	0.3082	0.3352
25	1	1.3280	1.2229	20.1000	18.0771	18.0000	18.0039	0.0125	0.0457	0.0353	0.3103	0.3376
26	1	1.2616	1.1164	20.1000	18.1836	18.1000	18.1043	0.0125	0.0440	0.0347	0.3126	0.3400
27	1	1.1939	1.0156	20.1000	18.2844	18.2000	18.2043	0.0125	0.0423	0.0337	0.3151	0.3426
28	1	1.1244	0.9185	20.1000	18.3815	18.3000	18.3042	0.0125	0.0406	0.0326	0.3179	0.3453
29	1	1.0525	0.8239	20.1000	18.4761	18.4000	18.4039	0.0125	0.0388	0.0312	0.3211	0.3482
30	1	0.9782	0.7309	20.1000	18.5691	18.5000	18.5035	0.0125	0.0370	0.0298	0.3247	0.3513
31	1	0.8812	0.6151	20.1000	18.6849	18.7000	18.6992	0.0125	0.0345	0.0262	0.3300	0.3558

32	1	0.7530	0.4706	20.1000	18.8294	18.9000	18.8964	0.0125	0.0313	0.0218	0.3384	0.3624
33	1	0.6028	0.3098	20.1000	18.9902	19.1000	19.0944	0.0125	0.0276	0.0187	0.3513	0.3716
34	1	0.4353	0.1370	20.1000	19.1630	19.3000	19.2930	0.0125	0.0234	0.0166	0.3723	0.3849
35	1	0.3002	0.0013	20.1000	19.2987	19.5000	19.4897	0.0125	0.0200	0.0179	0.3999	0.4000
36	-1	0.3002	0.0013	20.1000	19.2987	19.7000	19.4897	0.0125	0.0200	0.0179	0.3999	0.4000
37	-1	-0.3268	0.0000	20.1000	19.9218	19.9000	19.9000	0.0050	0.0043	0.0043	0.4000	0.4000
38	-1	-0.5000	0.0000	20.1000	20.1000	20.1000	20.1000	0.0000	0.0000	0.0000	0.4000	0.4000
39	-1	-0.6735	0.0000	20.1000	20.2786	20.3000	20.3000	-.0050	-.0043	-.0043	0.4000	0.4000
40	-1	-0.8472	0.0000	20.1000	20.4576	20.5000	20.5000	-.0100	-.0087	-.0087	0.4000	0.4000
41	-1	-0.3263	0.0000	20.1000	19.9210	19.9000	19.9000	0.0050	0.0043	0.0043	0.4000	0.4000
42	-1	-0.2400	0.0000	20.1000	19.8323	19.8000	19.8000	0.0075	0.0065	0.0065	0.4000	0.4000
43	-1	-0.1534	0.0000	20.1000	19.7433	19.7000	19.7000	0.0100	0.0087	0.0087	0.4000	0.4000
44	-1	-0.0669	0.0000	20.1000	19.6544	19.6000	19.6000	0.0125	0.0108	0.0108	0.4000	0.4000
45	-1	0.0195	0.0000	20.1000	19.5656	19.5000	19.5000	0.0150	0.0130	0.0130	0.4000	0.4000
46	-1	0.1058	0.0000	20.1000	19.4769	19.4000	19.4000	0.0175	0.0151	0.0151	0.4000	0.4000
47	-1	0.1921	0.0000	20.1000	19.3882	19.3000	19.3000	0.0200	0.0173	0.0173	0.4000	0.4000
48	-1	0.2783	0.0000	20.1000	19.2997	19.2000	19.2000	0.0225	0.0195	0.0195	0.4000	0.4000
49	1	0.3000	0.0000	20.1000	19.2775	19.1745	19.2166	0.0125	0.0200	0.0200	0.4000	0.4000
50	1	0.3613	0.0619	20.1000	19.2381	19.0000	19.0121	0.0125	0.0215	0.0220	0.3857	0.3925
51	1	0.4348	0.1368	20.1000	19.1632	18.9000	18.9134	0.0125	0.0234	0.0250	0.3724	0.3850
52	1	0.5105	0.2148	20.1000	19.0852	18.8000	18.8145	0.0125	0.0253	0.0278	0.3617	0.3784
53	1	0.5869	0.2947	20.1000	19.0053	18.7000	18.7156	0.0125	0.0272	0.0306	0.3529	0.3727
54	1	0.6631	0.3758	20.1000	18.9242	18.6000	18.6165	0.0125	0.0291	0.0332	0.3456	0.3676
55	1	0.7385	0.4581	20.1000	18.8419	18.5000	18.5174	0.0125	0.0310	0.0357	0.3395	0.3632
56	1	0.8126	0.5412	20.1000	18.7588	18.4000	18.4183	0.0125	0.0328	0.0380	0.3343	0.3592
57	1	0.8850	0.6251	20.1000	18.6749	18.3000	18.3191	0.0125	0.0346	0.0403	0.3297	0.3556
58	1	0.9554	0.7097	20.1000	18.5903	18.2000	18.2199	0.0125	0.0364	0.0424	0.3258	0.3523
59	1	1.0234	0.7950	20.1000	18.5050	18.1000	18.1207	0.0125	0.0381	0.0445	0.3224	0.3494
60	1	1.0887	0.8811	20.1000	18.4189	18.0000	18.0214	0.0125	0.0397	0.0465	0.3194	0.3467
61	1	1.1191	0.9199	20.1000	18.3801	18.1000	18.1143	0.0125	0.0405	0.0437	0.3181	0.3455
62	1	1.1050	0.8970	20.1000	18.4030	18.2000	18.2104	0.0125	0.0401	0.0384	0.3187	0.3460
63	1	1.0689	0.8474	20.1000	18.4526	18.3000	18.3078	0.0125	0.0392	0.0353	0.3203	0.3475
64	1	1.0179	0.7813	20.1000	18.5187	18.4000	18.4061	0.0125	0.0379	0.0328	0.3227	0.3496
65	1	0.9567	0.7055	20.1000	18.5945	18.5000	18.5048	0.0125	0.0364	0.0307	0.3258	0.3523
66	1	0.8881	0.6240	20.1000	18.6760	18.6000	18.6039	0.0125	0.0347	0.0288	0.3296	0.3554
67	1	0.8138	0.5391	20.1000	18.7609	18.7000	18.7031	0.0125	0.0328	0.0271	0.3342	0.3591
68	1	0.7353	0.4521	20.1000	18.8479	18.8000	18.8024	0.0125	0.0309	0.0254	0.3397	0.3634
69	1	0.6533	0.3638	20.1000	18.9362	18.9000	18.9018	0.0125	0.0288	0.0238	0.3465	0.3683
70	1	0.5686	0.2746	20.1000	19.0254	19.0000	19.0013	0.0125	0.0267	0.0223	0.3549	0.3740
71	1	0.5211	0.2254	20.1000	19.0746	18.9500	18.9564	0.0125	0.0255	0.0234	0.3604	0.3776
72	1	0.5174	0.2218	20.1000	19.0782	18.9000	18.9091	0.0125	0.0254	0.0253	0.3608	0.3779
73	1	0.5357	0.2408	20.1000	19.0592	18.8500	18.8607	0.0125	0.0259	0.0267	0.3586	0.3764
74	1	0.5652	0.2717	20.1000	19.0283	18.8000	18.8116	0.0125	0.0266	0.0280	0.3552	0.3742
75	1	0.6000	0.3083	20.1000	18.9917	18.7500	18.7623	0.0125	0.0275	0.0292	0.3516	0.3718
76	1	0.6372	0.3477	20.1000	18.9523	18.7000	18.7129	0.0125	0.0284	0.0304	0.3480	0.3693
77	1	0.6753	0.3887	20.1000	18.9113	18.6500	18.6633	0.0125	0.0294	0.0316	0.3446	0.3669
78	1	0.7138	0.4304	20.1000	18.8696	18.6000	18.6138	0.0125	0.0303	0.0327	0.3414	0.3646
79	1	0.7522	0.4726	20.1000	18.8274	18.5500	18.5641	0.0125	0.0313	0.0338	0.3385	0.3624
80	1	0.7903	0.5152	20.1000	18.7848	18.5000	18.5145	0.0125	0.0323	0.0349	0.3358	0.3603

C ***

Simulation results for Model 2 -- unsatseep#23_results_2019.mp

DAY	JUNSAT	HCI	ZF	HSTAGE	ZRF	HF	HFRP	AISRP	AIS	VRECH	WCI	WC
0	-1	-0.5000	0.0000	20.1000	20.0000	20.7000	20.7000	-.0130	-.0130	-.0130	0.4000	0.4000
1	-1	-0.8477	0.0000	20.1000	20.4584	20.5000	20.5000	-.0100	-.0087	-.0087	0.4000	0.4000
2	-1	-0.6737	0.0000	20.1000	20.2790	20.3000	20.3000	-.0050	-.0043	-.0043	0.4000	0.4000
3	-1	-0.5000	0.0000	20.1000	20.1000	20.1000	20.1000	0.0000	0.0000	0.0000	0.4000	0.4000
4	-1	-0.3265	0.0000	20.1000	19.9214	19.9000	19.9000	0.0050	0.0043	0.0043	0.4000	0.4000
5	-1	-0.1533	0.0000	20.1000	19.7431	19.7000	19.7000	0.0100	0.0087	0.0087	0.4000	0.4000
6	-1	0.0197	0.0000	20.1000	19.5653	19.5000	19.5000	0.0150	0.0130	0.0130	0.4000	0.4000
7	-1	0.1923	0.0000	20.1000	19.3878	19.3000	19.3000	0.0200	0.0173	0.0173	0.4000	0.4000
8	1	0.3000	0.0000	20.1000	19.2774	19.1749	19.1812	0.0125	0.0200	0.0200	0.4000	0.4000
9	1	0.3030	0.0030	20.1000	19.2970	18.9000	18.9202	0.0125	0.0201	0.0201	0.3992	0.3996
10	1	0.5005	0.1673	20.1000	19.1327	18.7000	18.7221	0.0125	0.0250	0.0285	0.3630	0.3792
11	1	0.7323	0.3451	20.1000	18.9549	18.5000	18.5232	0.0125	0.0308	0.0397	0.3400	0.3641

12	1	0.9255	0.5103	20.1000	18.7897	18.3000	18.3250	0.0125	0.0356	0.0461	0.3274	0.3553
13	1	1.0900	0.6765	20.1000	18.6235	18.1000	18.1267	0.0125	0.0397	0.0513	0.3194	0.3492
14	1	1.2250	0.8480	20.1000	18.4520	17.9000	17.9282	0.0125	0.0431	0.0557	0.3139	0.3446
15	1	1.3259	1.0242	20.1000	18.2758	17.7000	17.7294	0.0125	0.0456	0.0591	0.3104	0.3410
16	1	1.3954	1.2134	20.1000	18.0866	17.5000	17.5299	0.0125	0.0474	0.0623	0.3081	0.3379
17	1	1.4328	1.3839	20.1000	17.9161	17.3000	17.3314	0.0125	0.0483	0.0621	0.3070	0.3356
18	1	1.4523	1.5386	20.1000	17.7614	17.1000	17.1337	0.0125	0.0488	0.0616	0.3064	0.3338
19	1	1.4656	1.7519	20.1000	17.5481	16.9000	16.9331	0.0125	0.0491	0.0667	0.3060	0.3318
20	1	1.4717	1.9439	20.1000	17.3561	16.7000	16.7335	0.0125	0.0493	0.0655	0.3059	0.3302
21	1	1.4705	1.8208	20.1000	17.4792	17.6000	17.5938	0.0125	0.0493	0.0400	0.3059	0.3306
22	1	1.4613	1.5850	20.1000	17.7150	17.7000	17.7008	0.0125	0.0490	0.0295	0.3062	0.3326
23	1	1.4484	1.4556	20.1000	17.8444	17.8000	17.8023	0.0125	0.0487	0.0376	0.3065	0.3342
24	1	1.4262	1.3072	20.1000	17.9928	17.9000	17.9047	0.0125	0.0482	0.0360	0.3072	0.3361
25	1	1.3977	1.1914	20.1000	18.1086	18.0000	18.0055	0.0125	0.0474	0.0380	0.3081	0.3378
26	1	1.3697	1.1092	20.1000	18.1908	18.1000	18.1046	0.0125	0.0467	0.0401	0.3089	0.3392
27	1	1.3243	1.0015	20.1000	18.2985	18.2000	18.2050	0.0125	0.0456	0.0372	0.3104	0.3411
28	1	1.2698	0.9034	20.1000	18.3966	18.3000	18.3049	0.0125	0.0442	0.0366	0.3123	0.3431
29	1	1.2047	0.8073	20.1000	18.4927	18.4000	18.4047	0.0125	0.0426	0.0353	0.3147	0.3453
30	1	1.1294	0.7133	20.1000	18.5867	18.5000	18.5044	0.0125	0.0407	0.0338	0.3177	0.3479
31	1	1.0236	0.5989	20.1000	18.7011	18.7000	18.7001	0.0125	0.0381	0.0299	0.3224	0.3516
32	1	0.8725	0.4583	20.1000	18.8417	18.9000	18.8970	0.0125	0.0343	0.0248	0.3305	0.3575
33	1	0.6816	0.3031	20.1000	18.9969	19.1000	19.0947	0.0125	0.0295	0.0201	0.3440	0.3669
34	1	0.4568	0.1336	20.1000	19.1664	19.3000	19.2932	0.0125	0.0239	0.0162	0.3690	0.3829
35	-1	0.3000	0.0000	20.1000	19.3000	19.5000	19.5000	0.0150	0.0200	0.0177	0.4000	0.4000
36	-1	-0.1538	0.0000	20.1000	19.7439	19.7000	19.7000	0.0100	0.0087	0.0087	0.4000	0.4000
37	-1	-0.3268	0.0000	20.1000	19.9218	19.9000	19.9000	0.0050	0.0043	0.0043	0.4000	0.4000
38	-1	-0.5000	0.0000	20.1000	20.1000	20.1000	20.1000	0.0000	0.0000	0.0000	0.4000	0.4000
39	-1	-0.6735	0.0000	20.1000	20.2786	20.3000	20.3000	-.0050	-.0043	-.0043	0.4000	0.4000
40	-1	-0.8472	0.0000	20.1000	20.4576	20.5000	20.5000	-.0100	-.0087	-.0087	0.4000	0.4000
41	-1	-0.3263	0.0000	20.1000	19.9210	19.9000	19.9000	0.0050	0.0043	0.0043	0.4000	0.4000
42	-1	-0.2400	0.0000	20.1000	19.8323	19.8000	19.8000	0.0075	0.0065	0.0065	0.4000	0.4000
43	-1	-0.1534	0.0000	20.1000	19.7433	19.7000	19.7000	0.0100	0.0087	0.0087	0.4000	0.4000
44	-1	-0.0669	0.0000	20.1000	19.6544	19.6000	19.6000	0.0125	0.0108	0.0108	0.4000	0.4000
45	-1	0.0195	0.0000	20.1000	19.5656	19.5000	19.5000	0.0150	0.0130	0.0130	0.4000	0.4000
46	-1	0.1058	0.0000	20.1000	19.4769	19.4000	19.4000	0.0175	0.0151	0.0151	0.4000	0.4000
47	-1	0.1921	0.0000	20.1000	19.3882	19.3000	19.3000	0.0200	0.0173	0.0173	0.4000	0.4000
48	-1	0.2783	0.0000	20.1000	19.2997	19.2000	19.2000	0.0225	0.0195	0.0195	0.4000	0.4000
49	1	0.3000	0.0000	20.1000	19.2775	19.1745	19.1809	0.0125	0.0200	0.0200	0.4000	0.4000
50	1	0.3030	0.0030	20.1000	19.2970	19.0000	19.0151	0.0125	0.0201	0.0201	0.3992	0.3996
51	1	0.4182	0.1038	20.1000	19.1962	18.9000	18.9151	0.0125	0.0230	0.0244	0.3751	0.3865
52	1	0.5387	0.1960	20.1000	19.1040	18.8000	18.8155	0.0125	0.0260	0.0292	0.3583	0.3762
53	1	0.6503	0.2804	20.1000	19.0196	18.7000	18.7163	0.0125	0.0288	0.0329	0.3468	0.3687
54	1	0.7544	0.3622	20.1000	18.9378	18.6000	18.6172	0.0125	0.0314	0.0360	0.3383	0.3630
55	1	0.8519	0.4435	20.1000	18.8565	18.5000	18.5182	0.0125	0.0338	0.0388	0.3317	0.3584
56	1	0.9432	0.5254	20.1000	18.7746	18.4000	18.4191	0.0125	0.0361	0.0415	0.3265	0.3546
57	1	1.0281	0.6082	20.1000	18.6918	18.3000	18.3200	0.0125	0.0382	0.0439	0.3222	0.3514
58	1	1.1060	0.6922	20.1000	18.6078	18.2000	18.2208	0.0125	0.0402	0.0461	0.3187	0.3487
59	1	1.1763	0.7774	20.1000	18.5226	18.1000	18.1216	0.0125	0.0419	0.0481	0.3158	0.3463
60	1	1.2383	0.8637	20.1000	18.4363	18.0000	18.0222	0.0125	0.0435	0.0499	0.3134	0.3442
61	1	1.2641	0.9015	20.1000	18.3985	18.1000	18.1152	0.0125	0.0441	0.0470	0.3125	0.3433
62	1	1.2388	0.8581	20.1000	18.4419	18.2000	18.2123	0.0125	0.0435	0.0403	0.3134	0.3442
63	1	1.2140	0.8228	20.1000	18.4771	18.3000	18.3090	0.0125	0.0428	0.0402	0.3143	0.3450
64	1	1.1643	0.7563	20.1000	18.5437	18.4000	18.4073	0.0125	0.0416	0.0367	0.3163	0.3467
65	1	1.1015	0.6823	20.1000	18.6177	18.5000	18.5060	0.0125	0.0400	0.0346	0.3189	0.3488
66	1	1.0261	0.6023	20.1000	18.6977	18.6000	18.6050	0.0125	0.0382	0.0325	0.3223	0.3515
67	1	0.9399	0.5193	20.1000	18.7807	18.7000	18.7041	0.0125	0.0360	0.0303	0.3267	0.3547
68	1	0.8442	0.4348	20.1000	18.8652	18.8000	18.8033	0.0125	0.0336	0.0280	0.3322	0.3587
69	1	0.7405	0.3497	20.1000	18.9503	18.9000	18.9026	0.0125	0.0310	0.0258	0.3393	0.3637
70	1	0.6299	0.2641	20.1000	19.0359	19.0000	19.0018	0.0125	0.0282	0.0235	0.3487	0.3700
71	1	0.5656	0.2159	20.1000	19.0841	18.9500	18.9568	0.0125	0.0266	0.0243	0.3552	0.3742
72	1	0.5770	0.2246	20.1000	19.0754	18.9000	18.9089	0.0125	0.0269	0.0273	0.3540	0.3735
73	1	0.5943	0.2376	20.1000	19.0624	18.8500	18.8608	0.0125	0.0274	0.0280	0.3522	0.3723
74	1	0.6121	0.2511	20.1000	19.0489	18.8000	18.8127	0.0125	0.0278	0.0285	0.3504	0.3711
75	1	0.6305	0.2650	20.1000	19.0350	18.7500	18.7645	0.0125	0.0283	0.0290	0.3486	0.3699
76	1	0.7056	0.3232	20.1000	18.9768	18.7000	18.7141	0.0125	0.0301	0.0333	0.3421	0.3655
77	1	0.7267	0.3396	20.1000	18.9604	18.6500	18.6658	0.0125	0.0307	0.0316	0.3404	0.3644

78	1	0.8028	0.4017	20.1000	18.8983	18.6000	18.6152	0.0125	0.0326	0.0363	0.3349	0.3606
79	1	0.8269	0.4214	20.1000	18.8786	18.5500	18.5668	0.0125	0.0332	0.0344	0.3333	0.3595
80	1	0.8979	0.4837	20.1000	18.8163	18.5000	18.5161	0.0125	0.0349	0.0390	0.3290	0.3564

Peer-review history:
The peer review history for this paper can be accessed here:
http://www.sdiarticle4.com/review-history/56687